An Anderson impurity in conjugated polymers. II. Single-soliton solutions by the unrestricted Hartree-Fock approximation

1991 J. Phys.: Condens. Matter 3 4857

(http://iopscience.iop.org/0953-8984/3/26/008)

J. Phys.: Condens. Matter 3 (1991) 4857–4868. Printed in the UK

An Anderson impurity in conjugated polymers: II. Single-soliton solutions by the unrestricted Hartree–Fock approximation

Kikuo Harigaya†
Department of Physics, Faculty of Science, University of Tokyo, Hongo 7-3-1, Bunkyo-ku, Tokyo 113, Japan

Received 7 December 1990

Abstract. In order to investigate electronic structures around a carbonyl defect (>C=O), a dopant or an atomic side group in conjugated polymers, an Anderson impurity model is introduced in the Su–Schrieffer–Heeger (SSH) model. The case where the local level of the impurity has negative energy is considered. The Coulomb interaction term is treated by the unrestricted Hartree–Fock approximation. Polymer chains with odd sites are numerically diagonalized. Electron number is first taken to be half-filled. Next, it is increased by unity. In the half-filled case, the soliton is positively charged when two effective impurity levels are deep in the valence band. The impurity level is almost full. The mid-gap state of the soliton is nearly empty. As the Coulomb strength intensifies, the soliton gradually changes into a neutral (spin) soliton where one of the effective levels is high in the conduction band. The impurity levels are nearly singly occupied. When one electron is added, the change of the electronic states can be understood from that of the half-filled case. When the two effective levels are deep enough, the soliton is nearly neutral. If one of them is high in the conduction band, the soliton is negatively charged. A local moment does not exist for small Coulomb strengths U when electronic states are half-filled. It is present when an electron is added. This contrast is due (at $U = 0$) to whether the Fermi level is located in the gap or at one of the energy levels. Relations of the results to real defect states are discussed.

1. Introduction

When an impurity is present in conjugated polymers, electronic levels change drastically around the impurity. We have been studying the effects of three types of impurities in a series of publications [1–10]. The first one is the bond-type impurity [1, 2], which locally changes the electron-hopping integral. It has been found that bond-type impurities do not make an impurity band in the electronic Peierls gap. The second one is the site-type impurity [1, 3, 7], where the electronic site energy varies. Site-type impurities make an impurity band in the gap. It is located at an energy close to the valence or conduction band. The position depends on the sign of the impurity strength. Finally, the third one is the Anderson impurity discussed in the preceding paper (referred to as I hereafter) [10]. The Anderson impurity takes into account the cases where interactions between a

† Present address: Fundamental Physics Section, Physical Science Division, Electrotechnical Laboratory, Umezono 1-1-4, Tsukuba 305, Ibaraki, Japan.

0953-8984/91/264857 + 12 $03.50

polymer chain and an additional localized level are strong. Possible situations where the Anderson impurity model might be applied are: electron-hopping process between a dopant atom and a polymer chain; a local carbonyl (>C=O) defect that is naturally present in pristine polyacetylene; and the effects of an atomic side group that strongly accepts electrons from or donates them to the chain. We note that Mizes and Conwell [11] have independently proposed the use of the Anderson model (with no Coulomb interactions) to describe a carbonyl (>C=O) defect. The π bond between the carbon and the oxygen is modelled by the mixing interaction. We also note that Förner *et al* [12] have included the carbonyl defect by the modulation of the site energy. The present treatment is a generalization of their model. In I, we have studied the effects of an impurity without the Coulomb term. A new localized level has been found in the Peierls gap. This level is located above the top of the valence band if the impurity level is deep in the valence band. It is below the bottom of the conduction band when the impurity level is high enough in the conduction band. This level always exists whether the system is nearly dimerized or there is a soliton excitation pinned at the impurity.

We depict our model system schematically in figure 1. We consider an imaginary side atom, namely 'X', adjacent to a carbon atom of a polymer chain. In the atom X, there is one localized level in which Coulomb repulsion between electrons might be strong enough. In contrast, the Coulomb force in the chain would be relatively weak. We neglect it. As the atom X and the chain interact strongly via the mixing interaction, electronic states of the polymer chain would be drastically changed around the atom X. There would be an effective site-type impurity at the atom X.

Interactions between the atom X and the chain would indeed be quite interesting. When the atom X attracts electrons strongly and thus a local level, namely E_d, of the atom X is deep enough, the pristine configuration in figure 1(a) would change into configurations in figures 1(b)–(d). As the X atom would act as an effective site-type impurity, it would be energetically favourable to create a pinned soliton around the atom X. Figures 1(b) and (d) are the cases where the Coulomb force is weak, while it is sufficiently strong in figures 1(c) and (e). In figure 1(b), two electrons occupy the localized level and π-electronic states in the chain are filled with electrons, the number of which is reduced by unity from half-filling. A positively charged soliton is pinned at the site adjacent to the atom X. As the Coulomb repulsion becomes stronger, the number of localized electrons decreases. There might be one electron at the atom X when one of the effective levels is in the conduction band (the other remains in the valence band). The situation is depicted in figure 1(c). The soliton's mid-gap level is singly occupied and a spin soliton is present. Electronic level structures are different between figures 1(b) and (c). Crossover between the two cases may be described as a phase transition in a mean-field approximation [13]. A similar crossover may also occur when electron number changes. The case where electron number increases by unity is shown in figures 1(d) and (e). In figure 1(d), a spin soliton is pinned at the atom X. It might be transformed into a negatively charged soliton (figure 1(e)) as the Coulomb strength increases. In this way, our system may show fertile changes of electronic structures, which depend on given parameters, for example, filling of electrons and Coulomb interaction strength.

The Anderson impurity in metals was thoroughly investigated. It is now well known that the Kondo effect occurs. One of the causes of this effect is the singularity at the Fermi energy. Many-body effects strongly renormalize physical properties. Differently from the Anderson impurity in metals, the Fermi energy lies in the wide Peierls gap in the present system. It would be an interesting problem to clarify how the Kondo effect changes. But, in this paper, we do not discuss the possibility of the Kondo effect. We

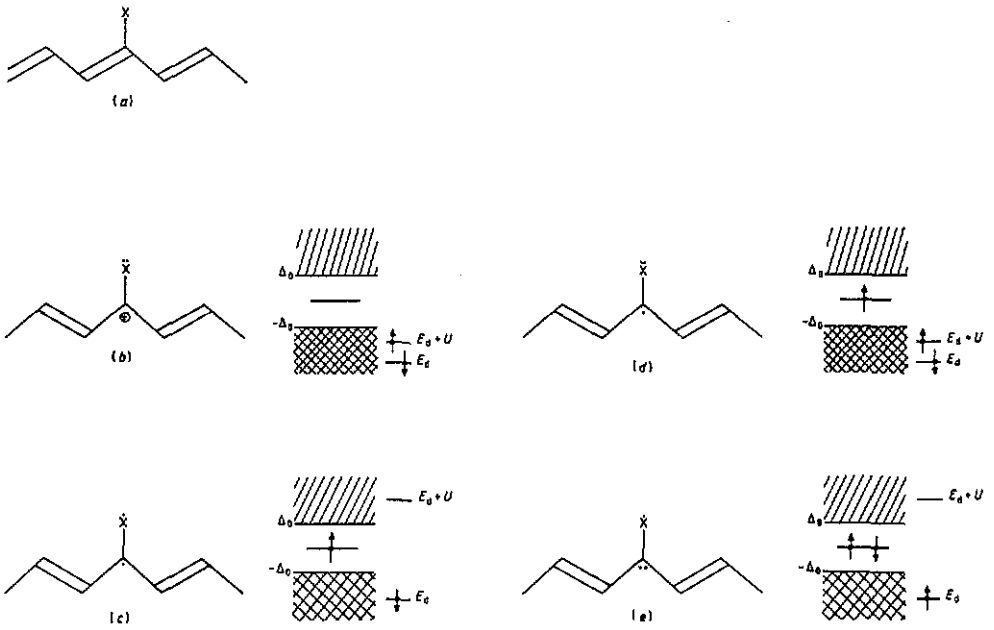

Figure 1. Schematic structures of an Anderson impurity in conjugated polymers. Electronic level structures are also shown. In (*a*), a pristine configuration with the nearly dimerized chain is shown. An Anderson impurity is denoted by the atom 'X'. In (*b*) and (*c*), the cases with half-filled electrons are shown. In (*d*) and (*e*), the cases where an electron is added are depicted. The two effective levels E_d and $E_d + U$ are deep in the valence band in (*b*) and (*d*). One of them, $E_d + U$, is in the conduction band in (*c*) and (*e*).

concentrate upon structures of one-electron states. Thus, we shall make use of the unrestricted Hartree–Fock (UHF) approximation for the Coulomb repulsion between electrons at the atom X. The Kondo effect is automatically excluded in the UHF.

The purpose of this paper is to investigate how lattice and electronic structures change, depending upon the impurity level, the Coulomb strength and the electron number. The case where the local level at the atom X has negative energy is considered. The Coulomb term has been treated by the UHF [13]. Polymer chains with odd sites are to be numerically diagonalized. First, electron number is taken to be half-filled (case A). Secondly, it is increased by unity (case B). Change of electronic structures, discussed in association with figure 1, is quantitatively investigated. In case A, the soliton is positively charged when two effective levels, E_d and $E_d + U$, are deep in the valence band. The d site is almost full. The mid-gap state of the soliton is nearly empty. As the Coulomb strength intensifies, the soliton gradually becomes a neutral (spin) soliton where one of the effective levels, $E_d + U$, is in the conduction band. The d level of the impurity is nearly singly occupied. In case B, change of the electronic levels can be understood from that of case A, by adding one electron. When the two effective levels are deep enough, the soliton is nearly neutral. If one of them is high in the conduction band, the soliton is nearly negatively charged. Relations to real defect states are discussed.

This paper is organized as follows. The model and the UHF treatment are explained in section 2. Section 3 is devoted to numerical results. We summarize the paper and give a discussion in section 4.

2. Model and numerical method

We consider the following model:

$$H = H_{\mathrm{SSH}} + H_{\mathrm{A}}. \tag{2.1}$$

The first term is the Su–Schrieffer–Heeger (SSH) Hamiltonian [14]

$$H_{\mathrm{SSH}} = -\sum_{n,s}[t_0 - \alpha(u_{n+1} - u_n)](c^{\dagger}_{n+1,s}c_{n,s} + \mathrm{HC}) + \tfrac{1}{2}K\sum_{n}(u_{n+1} - u_n)^2 \tag{2.2}$$

where t_0 is the nearest-neighbour hopping integral of the undimerized chain, α is the electron–phonon coupling strength due to the modulation of the hopping integral, u_n is the displacement of the nth CH unit, $c_{n,s}$ is an annihilation operator of an electron at the nth site with spin s ($s = \uparrow$ or $\downarrow$) and K is the force constant between adjacent units. The second term is the Anderson impurity [13] localized at the lth site

$$H_{\mathrm{A}} = E_{\mathrm{d}}\sum_{s} d^{\dagger}_{s}d_{s} + V\sum_{s}(d^{\dagger}_{s}c_{l,s} + c^{\dagger}_{l,s}d_{s}) + Ud^{\dagger}_{\uparrow}d_{\uparrow}d^{\dagger}_{\downarrow}d_{\downarrow} \tag{2.3}$$

where d_s is an annihilation operator of a localized electron at the atom X, E_{d} is its atomic level, V is the mixing matrix element between the localized level and the π-electron orbital at the lth site of the polymer chain and U is the on-site Coulomb repulsion strength at the atom X.

The model equation (2.1) is to be analysed with the help of the numerical diagonalization method. We use the UHF for the Coulomb interaction at the atom X. The Coulomb term in (2.3) is transformed as follows:

$$d^{\dagger}_{\uparrow}d_{\uparrow}d^{\dagger}_{\downarrow}d_{\downarrow} \Rightarrow \langle d^{\dagger}_{\uparrow}d_{\uparrow}\rangle d^{\dagger}_{\downarrow}d_{\downarrow} + d^{\dagger}_{\uparrow}d_{\uparrow}\langle d^{\dagger}_{\downarrow}d_{\downarrow}\rangle - \langle d^{\dagger}_{\uparrow}d_{\uparrow}\rangle\langle d^{\dagger}_{\downarrow}d_{\downarrow}\rangle. \tag{2.4}$$

We define charge and spin order parameters as

$$n = \langle d^{\dagger}_{\uparrow}d_{\uparrow}\rangle + \langle d^{\dagger}_{\downarrow}d_{\downarrow}\rangle \tag{2.5}$$

and

$$m = \langle d^{\dagger}_{\uparrow}d_{\uparrow}\rangle - \langle d^{\dagger}_{\downarrow}d_{\downarrow}\rangle \tag{2.6}$$

respectively. Then, equation (2.3) is transformed into

$$H'_{\mathrm{A}} = \sum_{s}\{E_{\mathrm{d}} + \tfrac{1}{2}[n + (\operatorname{sgn} s)m]U\}d^{\dagger}_{s}d_{s} + V\sum_{s}(d^{\dagger}_{s}c_{l,s} + c^{\dagger}_{l,s}d_{s}) - \tfrac{1}{4}(n^2 - m^2)U \tag{2.7}$$

where

$$\operatorname{sgn} s = \begin{cases} 1 & \text{if } s = \uparrow \\ -1 & \text{if } s = \downarrow. \end{cases}$$

In the UHF, wavefunctions are calculated by the Schrödinger equation:

$$\varepsilon_{\kappa,s}\varphi_{\kappa,s}(n) = -(t_0 - \alpha y_{n-1})\varphi_{\kappa,s}(n-1) - (t_0 - \alpha y_n)\varphi_{\kappa,s}(n+1) + V\delta_{n,l}\varphi_{\kappa,s}(d) \tag{2.8}$$

and

$$\varepsilon_{\kappa,s}\varphi_{\kappa,s}(d) = [E_d + \tfrac{1}{2}(n + (\operatorname{sgn} s)m)U]\varphi_{\kappa,s}(d) + V\varphi_{\kappa,s}(l). \tag{2.9}$$

The difference from I is that the wavefunctions depend on spin s. The bond variable is determined through

$$y_n = -\frac{2\alpha}{K}\sum_{\kappa,s}{}' \varphi_{\kappa,s}(n+1)\varphi_{\kappa,s}(n) + \frac{2\alpha}{KN}\sum_{m}\sum_{\kappa,s}{}' \varphi_{\kappa,s}(m+1)\varphi_{\kappa,s}(m). \tag{2.10}$$

Equations (2.5), (2.6), (2.8), (2.9) and (2.10) are to be solved numerically. The method is the same as in the previous papers [8–10].

3. Numerical results

Numerical results are reported for the parameters $\alpha = 4.1$ eV Å^{-1}, $K = 21$ eV Å^{-2} and $t_0 = 2.5$ eV with $N = 51$. These give $\lambda \equiv 2\alpha^2/\pi K t_0 = 0.20$. We particularly take $V = 0.5t_0$. The quantities E_d and U are taken as independent variables in order to see how the electronic structures of the chain system and the atom X change. They are varied within $-1.0t_0 \leqslant E_d \leqslant 0$ and $0 \leqslant U \leqslant 2.0t_0$. We specially consider the case $E_d < 0$ for simplicity. This case was shown in figure 1. Results for the case $E_d > 0$ can be obtained by performing charge conjugation transformation.

3.1. $N_e = N + 1$

In this subsection, we report on numerical results of the half-filled system, which means that the total number of states in the system is $2(N+1)$ and electron number is the half of $2(N+1)$. Electron numbers of the 'up' and 'down' spins are the same $N_\uparrow = N_\downarrow = 26$.

We show typical solutions when the d level is deep and in the valence band: $E_d = -0.6t_0$. When the Coulomb strength U is not too strong, the two effective levels, E_d and $E_d + U$, are located in the valence band. The situation was shown in figure 1(*b*). We present a typical solution for $U = 0.2t_0$. Figure 2(*a*) shows the smoothed bond variable $\bar{y}_n \equiv (-1)^n(y_n - y_{n+1})/2$. A pinned soliton is found around the impurity at $n = 25$. Figure 2(*b*) shows the smoothed charge density, $\bar{\rho}_n \equiv \Sigma_s(\langle c^\dagger_{n-1,s}c_{n-1,s}\rangle + 2\langle c^\dagger_{n,s}c_{n,s}\rangle + \langle c^\dagger_{n+1,s}c_{n+1,s}\rangle)/4$, together with the d-electron number n by the vertical line. The d level is filled up with about two electrons. The π-electron system has reduced electron density (excess hole density) around the impurity. Then, the soliton is positively charged. Figure 2(*c*) is the spin density distribution, $\bar{\sigma}_n \equiv \Sigma_s(\operatorname{sgn} s)(\langle c^\dagger_{n-1,s}c_{n-1,s}\rangle + 2\langle c^\dagger_{n,s}c_{n,s}\rangle + \langle c^\dagger_{n+1,s}c_{n+1,s}\rangle)/4$. There is no spin density. Energy levels are degenerate with respect to spin s. This is because the Fermi energy lies between occupied and unoccupied levels of the π-electron system. It would be energetically favourable to make m zero.

On the other hand, if one of the effective levels, $E_d + U$, is so large that it is in the conduction band, the electronic structure is different. Figure 3 shows a solution for $U = 1.8t_0$. As shown in figures 3(*b*) and (*c*), the order parameters, n and m, are about unity. This shows that one of the effective levels at the atom X is nearly full, and the other is almost empty. Then, a magnetic local moment appears at the d level in the mean-field picture of the Anderson impurity [13]. This moment was depicted in figure 1(*c*) by the point at the atom X. The π-electronic system has almost uniform charge distribution

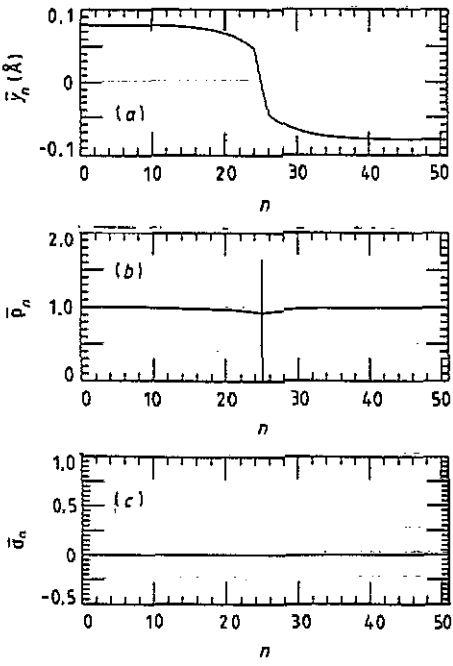

Figure 2. Dimerization pattern (a), electron density (b) and spin density (c) in the SSH model with an Anderson impurity at $n = 25$. In (b), electron number n at the d level is also shown by the vertical line. In (c), number of spin m at the d level is presented by the vertical line. Parameters are $V = 0.5t_0$, $E_d = -0.6t_0$, $U = 0.2t_0$, $N = 51$ and $N_e = 52$.

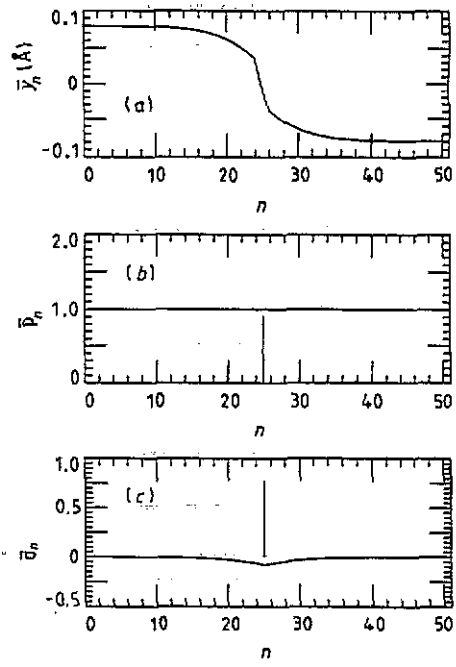

Figure 3. Dimerization pattern (a), electron density (b) and spin density (c) in the SSH model with an Anderson impurity at $n = 25$. In (b), electron number n at the d level is also shown by the vertical line. In (c), number of spin m at the d level is presented by the vertical line. Parameters are $V = 0.5t_0$, $E_d = -0.6t_0$, $U = 1.8t_0$, $N = 51$ and $N_e = 52$.

and the spin density changes around $n = 25$. So, the pinned soliton is a spin soliton. The mid-gap level is nearly singly occupied as shown in figure 1(c). Soliton width is larger in figure 3(a) than that in figure 2(a), because of weakening of the pinning force. The crossover between figures 2 and 3 is the second-order phase transition in the formalism of the UHF, which will be discussed later.

Figure 4 shows the energy level structure around the energy gap as a function of U with E_d ($= -0.6t_0$) kept constant. The Fermi energy is denoted by the broken curve. The thin curve indicates $E_d + U$. For $U < 1.0t_0$, the energies of the levels increase as U increases. The levels are doubly degenerate. The unoccupied level in the gap is the mid-gap level of the positive soliton. When $U > 1.0t_0$, each level splits into two undegenerate levels due to the phase transition. For $1.0t_0 < U \lesssim 1.1t_0$, the energy levels in the gap would be complicated mixed levels of the soliton's mid-gap state and the d level of the atom X. This would easily be suspected if we remind ourselves of the fact that the positive gradient of energy levels as a function of U is very close to that of the thin curve at $U = 1.0t_0$. When $U \gtrsim 1.1t_0$, there are two levels in the gap. One of them is occupied and the other is unoccupied. They are associated with the pinned spin soliton.

Changes of level structure in the gap are summarized in a phase diagram in figure 5. The quantities U and E_d are taken as variables. The thick curve is the boundary of the phase transition between $m = 0$ and $m \neq 0$. The character of localized levels also changes.

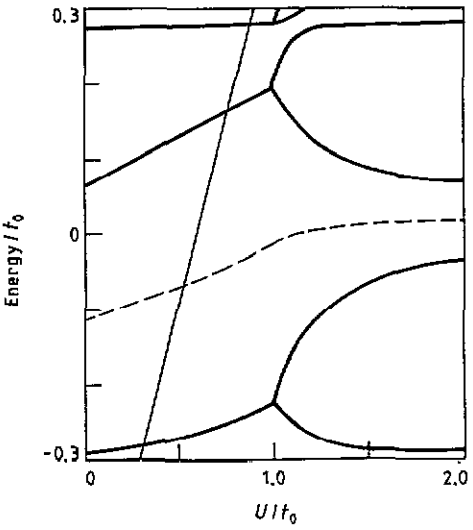

Figure 4. Electronic level structure around the Peierls gap as a function of U. Parameters are $V = 0.5t_0$, $E_d = -0.6t_0$, $N = 51$ and $N_e = 52$. The Fermi level is denoted by the broken curve. The thin line is the effective level $E_d + U$.

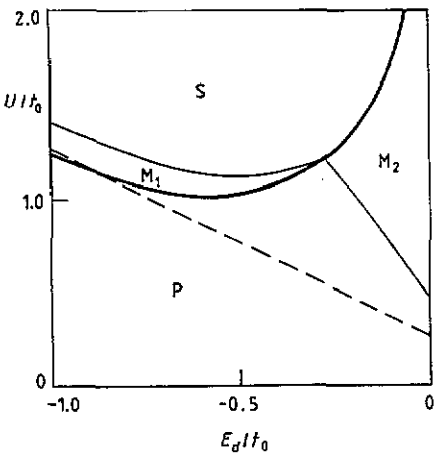

Figure 5. Phase diagram of electronic levels in the Peierls gap. Parameters are $V = 0.5t_0$, $N = 51$ and $N_e = 52$. The symbols P and S indicate that there are positive and spin solitons, respectively. The symbols M_j ($j = 1, 2$) mean that levels are mixed ones of the impurity level and the mid-gap state. M_1 is for $m \neq 0$ while M_2 is for $m \approx 0$. The heavy full curve is the boundary of the second-order phase transition. The broken line shows the relation $E_d + U = \Delta_0$.

The other thin curves are the boundaries where the character of localized levels located in the gap only changes. The region P is the phase where a positive soliton is present. The symbols M_1 and M_2 denote the regions where mixed energy levels of the mid-gap state and the d state are present. The region S is the phase with the spin soliton. When the d level is deep enough ($E_d < -0.28t_0$), the local moment is present in the region M_1. When $E_d > -0.28t_0$, the moment appears for larger U than in the region M_2. The symbols M_1 and M_2 indicate this difference. The broken line shows the relation $E_d + U = \Delta_0$. When E_d is deep enough ($E_d < -0.6t_0$), the two boundaries among the regions P, M_1 and S are nearly parallel to the broken line.

Figure 6 shows variations of n and m as a function of U with $E_d = -0.6t_0$. For small U, n decreases linearly. This reflects the upward shift of one of the effective levels. For larger U, n ceases decreasing as m increases. This means development of the local moment at the d level.

Figure 7 shows the boundary between the phases $m = 0$ and $m \neq 0$ in the E_d/U versus U^{-1} plane. The curve has a maximum near $E_d/U = -0.5$. This is due to the electron–hole symmetry of the mean-field Hamiltonian when $E_d = -\frac{1}{2}U$. This property is the same as in the UHF solution of the Anderson impurity in metals [13]. The value of U^{-1} at the maximum corresponds to $\pi\Gamma/U = 0.393$, where $\Gamma \equiv V^2/2t_0$ is the broadening of the d level, obtained from equation (3.7) in I. For the Anderson impurity in metals, the maximum value is 1.0 [13]. The two values do not agree. This might be due to the finite system size and/or the effect of the presence of the wide energy gap.

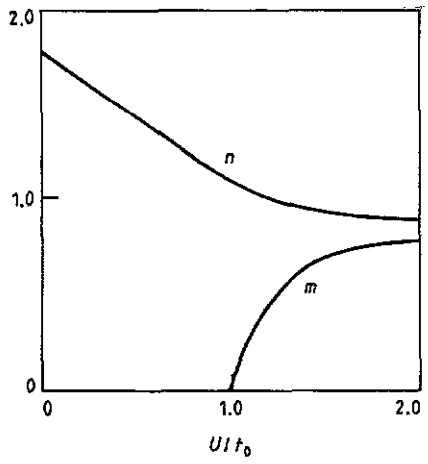

Figure 6. Variation of order parameters m and n as a function of U. Parameters are $V = 0.5t_0$, $E_d = -0.6t_0$, $N = 51$ and $N_e = 52$.

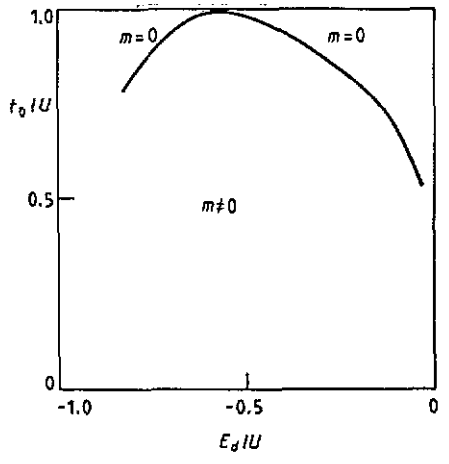

Figure 7. Phase boundary between the two phases with $m = 0$ and $m \neq 0$ in the E_d/U versus t_0/U plane.

3.2. $N_e = N + 2$

In this subsection, we present numerical results for systems where electron number increases by unity from that in section 3.1. We take $N_\uparrow = 27$ and $N_\downarrow = 26$. Typical solutions are presented for $E_d = -0.6t_0$. Figure 8 shows the case $E_d + U < -\Delta_0$. We specially take $U = 0.2t_0$. A soliton is weakly pinned around the impurity at $n = 25$, as shown in figure 8(a). Figure 8(b) shows that the d level is nearly doubly filled and the distribution of π electrons is almost uniform. Figure 8(c) shows that there is excess spin density around $n = 25$. So, the soliton is a spin soliton. This was shown in figure 1(d). Two points at the atom X represent the d electrons, the number of which is about two. In contrast to figure 2, the order parameter m is finite and energy levels are not degenerate with respect to spin s. The reason might be that the Fermi energy is located at the singly occupied mid-gap level if $m = 0$. Thus, it is energetically favourable to make m finite.

Figure 9 shows a typical solution for the case $E_d + U > \Delta_0$. We take $U = 1.8t_0$. In figure 9(a), the soliton is weakly pinned by the impurity at $n = 25$. The soliton width is larger than that in figure 8(a). Figure 9(b) shows the charge distribution. Filling of the d level is almost one. Excess π electrons cluster aound the impurity. Figure 9(c) is the spin density. There is a localized spin at the d level. The system of π electrons has almost no spin. Then, the soliton is a negatively charged one. As discussed in I, the effective site-type strength is positive. Thus, the pinning force of solitons is strongest for a positive soliton. It is weakest for a negative soliton. This explains well the variation of the soliton width.

Figure 10 shows the change of the energy level structure as a function of U with $E_d = -0.6t_0$ fixed. The Fermi energy is denoted by the broken curve. The thin line shows $E_d + U$. When $0 < U < 0.30t_0$, there are two levels in the gap. Each of them is not degenerate with respect to spin. The lower level is occupied and the upper one is unoccupied. They are associated with the spin soliton. When $0.30t_0 < U < 0.84t_0$, there are three levels in the gap. They are mixed levels originating from the two mid-gap levels and the upper effective level $E_d + U$. Finally, if $U > 0.84t_0$, both levels in the gap are

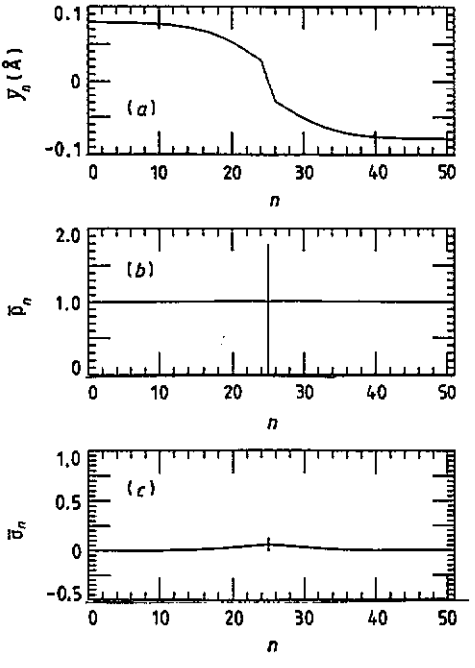

Figure 8. Dimerization pattern (*a*), electron density (*b*) and spin density (*c*) in the SSH model with an Anderson impurity at $n = 25$. In (*b*), electron number n at the d level is also shown by the vertical line. In (*c*), number of spin m at the d level is presented by the vertical line. Parameters are $V = 0.5t_0$, $E_d = -0.6t_0$, $U = 0.2t_0$, $N = 51$ and $N_e = 53$.

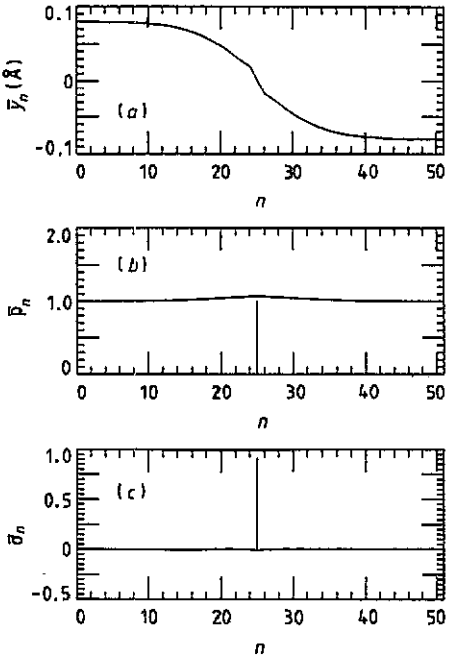

Figure 9. Dimerization pattern (*a*), electron density (*b*) and spin density (*c*) in the SSH model with an Anderson impurity at $n = 25$. In (*b*), electron number n at the d level is also shown by the vertical line. In (*c*), number of spin m at the d level is presented by the vertical line. Parameters are $V = 0.5t_0$, $E_d = -0.6t_0$, $U = 1.8t_0$, $N = 51$ and $N_e = 53$.

occupied. They are the mid-gap levels of the negative soliton. It should be noted that the two boundaries, $U = 0.30t_0$ and $0.84t_0$, are well explained by the relations $E_d + U = \pm\Delta_0$. When the upper effective level $E_d + U$ is in the Peierls gap, there are three mixed levels. On the other hand, when it is in the valence or conduction band, there are two levels.

We summarize the variation of electronic structure in the E_d versus U plane as a phase diagram. It is shown in figure 11. The full curves are boundaries where the number of levels in the gap changes. The broken lines indicate the relations $E_d + U = \pm\Delta_0$. The symbols S and N mean that there are spin and negative solitons, respectively. The region M indicates that energy levels are complicated mixed ones. The positions of the two full curves agree well with the two broken lines. It is noted that m does not vanish over all the space except along the line $U = 0$.

Variations of n and m are shown as a function of U in figure 12. We take $E_d = -0.6t_0$. The two quantities vary almost linearly when U is small. They increase weakly or decrease weakly when U is larger. The curve of n is similar to that in figure 6.

4. Summary and discussion

We have discussed how the Coulomb repulsion at the d site affects one-electron level structures when a soliton is present around the impurity. The case where the local level

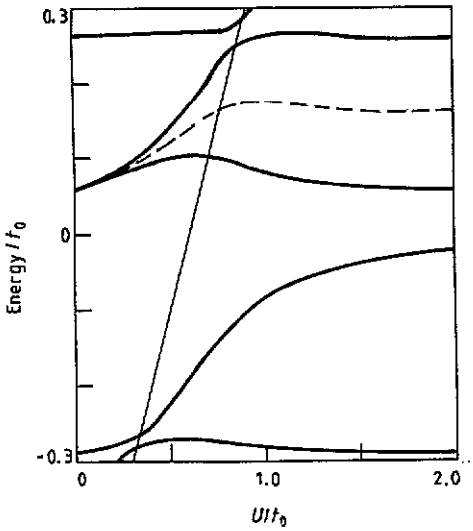

Figure 10. Electronic level structure around the Peierls gap as a function of U. Parameters are $V = 0.5t_0$, $E_d = -0.6t_0$, $N = 51$ and $N_e = 53$. The Fermi level is denoted by the broken curve. The thin line is the effective level $E_d + U$.

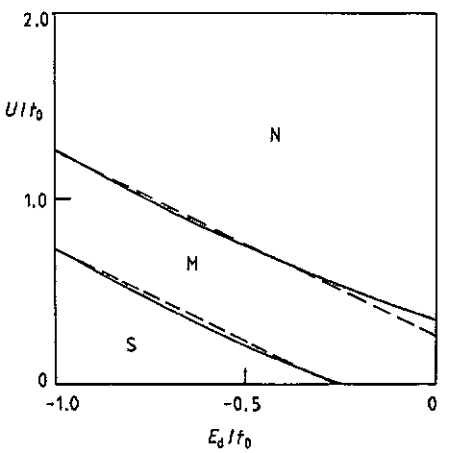

Figure 11. Phase diagram of electronic levels in the Peierls gap. Parameters are $V = 0.5t_0$, $N = 51$ and $N_e = 52$. The symbols N and S indicate that there are negative and spin solitons, respectively. The symbol M means that levels are mixed ones of the impurity level and the mid-gap state. The broken lines show the relations $E_d + U = \pm\Delta_0$.

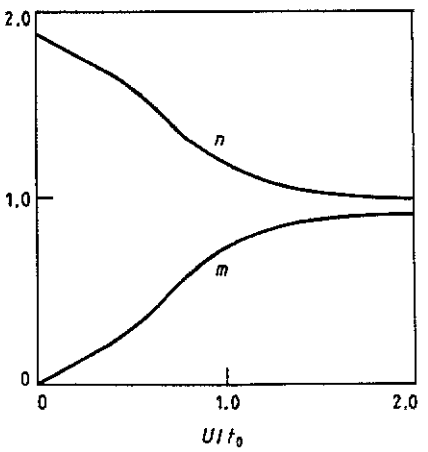

Figure 12. Variation of order parameters m and n as a function of U. Parameters are $V = 0.5t_0$, $E_d = -0.6t_0$, $N = 51$ and $N_e = 53$.

at the d site has negative energy has been considered. The Coulomb term has been treated by the UHF [13]. Polymer chains with odd sites have been numerically diagonalized. First, electron number has been taken to be half-filled (case A). Secondly, it is increased by unity (case B). In case A, the soliton is positively charged when two effective levels, E_d

and $E_d + U$, are deep in the valence band. The d site is almost full. The mid-gap state of the soliton is nearly empty. As the Coulomb strength intensifies, mixing between the localized level of the impurity and the mid-gap level becomes stronger. Finally, the soliton becomes a neutral (spin) soliton when one of the effective levels, $E_d + U$, is in the conduction band. The d level of the impurity is nearly singly occupied. In case B, the change of the level structures can be understood from that of case A by adding one electron. When the two effective levels are deep enough, the soliton is nearly neutral. If one of them is high in the conduction band, the soliton is nearly negatively charged. As the charge of the soliton goes from positive, through neutral, finally to negative, the width of the soliton extends. This is due to weakening of the pinning force.

When the Coulomb force is weak, there is no local moment for case A. It is present for case B. This contrast arises because (at $U = 0$) the Fermi level is located in the Peierls gap for case A, while it is just at the singly occupied level in case B. In case A, when the Coulomb strength intensifies, there occurs the second-order phase transition. The local moment appears for the larger U phase. The phase boundary in the E_d/U versus t_0/U plane is similar to that of the Anderson impurity in metals. It has a peak when $E_d \simeq -\frac{1}{2}U$, as seen in figure 7. This is due to the electron–hole symmetry [13]. When E_d is shallow, the phase boundary separates one of the mixed states and the spin soliton state. If E_d is deep, the boundary separates the positive soliton state and the other of the mixed states. This is clearly seen in figure 5. In case B, the transition from the positive soliton state, through the mixed state, to the negative soliton state is due to change of the position of the effective levels at the d site. The two boundaries in figure 11 coincide well with the relations $E_d + U = \pm\Delta_0$.

In view of the fertile change of electronic structures, it should be useful to remark on relations to realistic defect states. When the impurity is a carbonyl (>C═O) defect, the π electron of the carbon at the defect forms a π bond with the oxygen atom. There is a double bond between the carbon and the oxygen. This bond has been represented by the mixing interaction in our model. The localized d level should be nearly singly occupied. One effective level, E_d, must be in the valence band: $E_d < -\Delta_0$. The other level, $E_d + U$, is in the conduction band: $E_d + U > \Delta_0$. The number of π electrons of the carbon adjacent to the impurity is about unity. This electron is located at the defect that connects the two undegenerate ground states of the polymer chain. Thus, a neutral soliton is pinned at the impurity. This situation has been depicted in figure 1(*c*). This case corresponds to the local carbonyl state. In our mean-field result, localized spins are present at the soliton and the d site. Two states with respect to the two spins mix with each other to form a π bond between the carbon and the oxygen. The total spin is zero. This coincides with experiments: the carbonyl defect (>C═O) has no total spin. However, we cannot identify each spin experimentally. This may reveal the limitation of the mean-field theory. Large fluctuations neglected in the mean-field treatment may generate the singlet confinement of the two localized spins, as the recent numerical diagonalization study of the finite tight-binding system with Anderson impurity indicates [15]. Then, we would not be able to identify two spins at $T = 0$. This should be checked in future work.

When the defect is a dopant, electrons of the dopant make a full shell. The d level of our model is nearly full when the dopant is an acceptor. It is almost empty when the dopant is a donor. The two cases may be modelled by the parameters $U = 0$ and $|E_d| \gg \Delta_0$. This has been investigated in I. We have shown that the impurity is equivalent to the effective site-type impurity. The positive site-type impurity corresponds to an acceptor, while the negative one corresponds to a donor.

Finally, when the defect is an atomic side group, there may be many cases. Our data by the general treatment might correspond to various situations. It seems that our model is too simple to describe real defect states. However, we believe that variation of one-electron level structures are simulated well by the present calculations.

Acknowledgments

Numerical investigations have been performed on HITAC M-680 and S-820 of the Computer Center of the University of Tokyo, and also on HITAC M-680 and S-820 of the Institute of Molecular Science, Okazaki National Research Institutes.

References

[1] Harigaya K, Wada Y and Fesser K 1989 *Phys. Rev. Lett.* **63** 2401
[2] Harigaya K, Wada Y and Fesser K 1990 *Phys. Rev.* B **42** 1268
[3] Harigaya K, Wada Y and Fesser K 1990 *Phys. Rev.* B **42** 1276
[4] Harigaya K, Wada Y and Fesser K 1990 *Strongly Coupled Plasma Physics* ed S Ichimaru (Amsterdam: Elsevier; Tokyo: Yamada Science Foundation) p 255
[5] Harigaya K 1990 *J. Phys. Soc. Japan* **59** 1348
[6] Harigaya K, Wada Y and Fesser K 1990 *Phys. Rev. Lett.* **65** 806
[7] Harigaya K, Wada Y and Fesser K 1990 *Phys. Rev.* B **42** 11303
[8] Harigaya K, Terai A, Wada Y and Fesser K 1991 *Phys. Rev.* B **43** 4141
[9] Harigaya K and Terai A 1991 *Solid State Commun.* **78** 335
[10] Harigaya K 1991 *J. Phys.: Condens. Matter* **3** 4841
[11] Mizes H A and Conwell E M 1990 *Proc. Int. Conf. on Science and Technology of Synthetic Metals 1990* (to be published)
[12] Förner W, Seel M and Ladik J 1986 *Solid State Commun.* **57** 463
[13] Anderson P W 1961 *Phys. Rev.* **124** 41
[14] Su W-P, Schrieffer J R and Heeger A J 1980 *Phys. Rev.* B **22** 2099
[15] Yanagisawa T 1990 *Proc. 19th Int. Conf. on Low Temperature Physics (Physica* **165/166**) p 399; 1991 *J. Phys. Soc. Japan* **60** 29